Available online at www.sciencedirect.com
SCIENCE DIRECT®
International Journal of Heat and Mass Transfer 49 (2006) 815–824
International Journal of HEAT and MASS TRANSFER
www.elsevier.com/locate/ijhmt

Review

Characterization of liquid flows in microfluidic systems

Tuba Bayraktar [a,*], Srikanth B. Pidugu [b]

[a] Department of Chemical Engineering, School of Engineering and Technology, Hampton University, Hampton, VA 23668, United States
[b] Department of Engineering Technology, Donaghey College of Information Science and Systems Engineering, University of Arkansas at Little Rock, Little Rock, AR 72204, United States

Received 15 September 2005; received in revised form 8 November 2005
Available online 10 January 2006

Abstract

The microfluidic devices have recently attracted tremendous interest due to their potential of bringing novel applications into reality in many areas including biomedical industry. However, the challenges in the design of microfluidic devices still remain since all aspects of fluid flow in microchannels have not been yet fully understood. This paper presents major findings in the literature on fundamentals of flow physics in microchannels. The review is intended to provide an extensive overview on the available knowledge base as well as the areas that require intensive investigation. It includes studies on both pressure-driven and electro-osmotic flows in microchannels.

Keywords: Microchannels; Electroosmotic flows; Pressure measurements; Joule heating; Miniaturization

Contents

* Corresponding author. Tel.: +1 757 727 5557; fax: +1 757 727 5189.
E-mail address: tuba.bayraktar@hamptonu.edu (T. Bayraktar).

0017-9310/$ - see front matter
doi:10.1016/j.ijheatmasstransfer.2005.11.007

1. Introduction

Miniaturized devices have found application in many areas such as chemical processes, propulsion and power generation, cooling of electronic devices, aerospace industry, inkjet printers, and biomedical industry. The use of microfluidic devices in the biomedical industry has received recent attention due to several advantages of miniaturization. These advantages include: (1) low unit cost of microfluidic structures at mass production; (2) high throughput in parallel processing; (3) reduced volume of sample and reagent; (4) reduced volume of waste; and (5) possibility of the fabrication of highly integrated and disposable devices. New devices entitled "lab-on-a-chip" have been developed in order to produce integrated and mobile analysis systems. The long-term goal in this area is the production of lab-on-a-chip systems that will eliminate time-consuming clinical testing in central laboratories. The primary goal of the present paper is to provide a wide overview of findings on the underlying principles of microflow physics. The issues discussed include the effect of microchannel material and cross-section on flow behavior; pressure drop and friction measurements in microchannels; mixing and flow control methods for microfluidic systems; and visualization and velocimetry techniques for microflow. The Joule heating, which has an adverse effect in the performance of electro-kinetic systems, is also closely examined.

Although recent papers [1,2] have given reasons for conflicting results obtained by different researchers, it can be still concluded at this point of research that no agreement has been found among studies focusing on the characterization of friction factor/pressure drop for microflow systems. Further investigation requires understanding of how entrance effects differ for microflows from macro scale flow. There is a clear need to investigate the characteristics of non-Newtonian fluid flow in microchannels.

2. Theory of miniaturization

In case of microdevices, the continuum approach can still be applied for modeling fluid flow, especially if the fluid is liquid. However, there are many situations where fluid flow behavior in microdevices can considerably deviate from those in macroscopic devices. The characteristic dimension of a microchannel within a microfluidic system is in the range of 1–1000 μm. The Reynolds numbers encountered in microfluidic systems are quite small (often on the order of 1.0 or smaller). Surface forces, which originate due to intermolecular forces, could be important in microchannel flows. These forces are generally ignored at macro scale. Surface effects also alter the value of viscosity. It is found that the apparent viscosity is lower in the narrower channel, which is contrary to the expected trend [3]. Another important effect is air-dampening, which could directly influence quality factor of the devices. The strong air dampening is due to the dramatic increase in the surface-to-volume ratio. Due to large surface-to-volume ratios in microdevices, both convective and radiative heat transfer rates are enhanced considerably. Despite deviation of flow behavior at the microlevel, one should carefully analyze to see if the continuum approach is valid in a given microfluidic device. For example, a 10 μm thickness contains 30,000 water molecules, enough to treat a flow to be in continuum. In this section, we provide governing and auxiliary equations needed for analyzing flows in microdevices. The equations governing fluid flow, known as "Navier–Stokes equations," are conservation of mass, momentum, and energy and can be expressed in partial differential form as:

$$\frac{\partial \rho}{\partial t} + \frac{\partial \rho}{\partial x_i}(\rho u_i) = 0 \tag{1}$$

$$\frac{\partial}{\partial t}(\rho u_i) + \frac{\partial}{\partial x_i}(\rho u_j u_i) = \rho \mathbf{F}_i - \frac{\partial p}{\partial x_i} + \frac{\partial}{\partial x_j}\tau_{ji} \tag{2}$$

$$\frac{\partial}{\partial t}(\rho e) + \frac{\partial}{\partial x_i}(\rho u_i e) = -p\frac{\partial u_i}{\partial x_i} + \tau_{ji}\frac{\partial u_i}{\partial x_j} + \frac{\partial q_i}{\partial x_i} \tag{3}$$

In the above equations, u_i represents the flow velocity; ρ is the density; p is the pressure; τ is the stress tensor; e is the specific internal energy; $\mathbf{F}$ is the body force; and q is the heat flux. The repeated indices in any single term indicate a summation following a standard summation convention. The above equations do not form a closed system of equations, and one needs constitutive relationships among unknowns to achieve this task. The above equations can be simplified considerably for Newtonian and incompressible fluids. When a constant temperature assumption is valid, the energy equation can be de-coupled from mass and momentum equations, providing further simplifications. Flow in microchannels can be also achieved by means of application of electric fields. The above equations need to be modified to include the effects of the applied electric field forces, and relevant information is given in the next section.

2.1. Types of flows

Fluid is transported in several ways in the microchannels used in microfluidic devices. Two important methods of transport are flows driven by pressure differential and electro-osmotic flows. In the former case, flow is transported by means of applied pressure differences. In the latter case, flow transport is initiated by application of a high electric field. This type of flow is broadly classified as electro-kinetic flow. Capillary driving forces owing to surface tension, "wetting" of surfaces by the fluid, can also lead to pressure gradients in liquids. This pressure gradient causes flow transport, so it is similar in many ways to pressure-driven flows. However, the shape of the interface is an important factor in this type of flow. Free surface flows are caused by gradients in interfacial tension (Marangoni flows). These can be manipulated using the dependence of surface tension on temperature or chemical concentration.

Of all the four types of flows described above, electro-kinetic flows and pressure-driven flows are most widely studied. In microchannels, flows of common liquids are driven by typical electric fields (~100 V/cm) and mostly characterized by low values of the Reynolds number [4]. Both types of flows have advantages and disadvantages. Weigl et al. [5] indicated that both of these techniques are not ultimate solutions for the fluid transport and control due to some of their disadvantages. However, electro-kinetic flows offer an important advantage over pressure-driven flows in one aspect, that they provide uniform velocity profiles (i.e., velocity is constant everywhere in microchannel except very close to the wall), when a uniform distribution of charge is applied on the microchannel walls. This is termed as "perfect plug flow" and is characterized by dispersion that is dependent only on the molecular diffusion constant of the sample, which allows low sample dispersion [6,7]. One of the reasons that electro-kinetic flow is so often used in microfluidics is that much lower sample dispersions can be achieved compared with pressure-driven pumping [8]. Electrokinetic flows also obviate the necessity of having moving parts in a microfluidic system. Another advantage of electro-kinetic flows is that they can be used in applications where separation of mixtures is important, though it is not good for general transport. Electrokinetic flows offer an advantage when dealing with the flows in interconnected or branched channels. Such flows can be easily controlled by switching voltages without the need of valves. However, electro-kinetic flows also have some disadvantages. The main disadvantage is that this type of flow is limited to polar solvents. They are characterized by high electric field requirements (>100 V/cm) and low flow speeds (<1 mm/s). Electrokinetic flows are highly sensitive to surface contamination.

The elektrokinetic phenomenon has been known since the early 19th century. Burgreen and Nakache [9] and Probstein [10] briefly reviewed the historical development of the elektrokinetic theory. Electrokinetic flows are classified into the following four types: electrophoresis, electro-osmosis, streaming potential, and sedimental potential. This paper mainly focuses on electrophoresis and electro-osmosis, both requiring an applied electric field to create motion. In case of electrophoresis, charged particles move relative to the stationary liquid by the application of an electric field; whereas, in the case of electroosmosis, ionized liquid moves relative to the stationary charged surface by action of the applied electric field. The early studies on the elektrokinetic theory mostly examined the electro-osmotic velocity distribution in fine capillaries [9,11].

When a charged solid surface and a polar medium are in contact, the surface charge influences the distribution of the ions within the liquid near the solid surface. The counterions in the liquid are attracted toward the surface and coions are repelled from the surface. The electric double layer (EDL) is the region formed by the excess counterions in the liquid. The EDL consists of two regions: the Stern layer and diffuse (or Gouy–Chapman) layer (see Fig. 1).

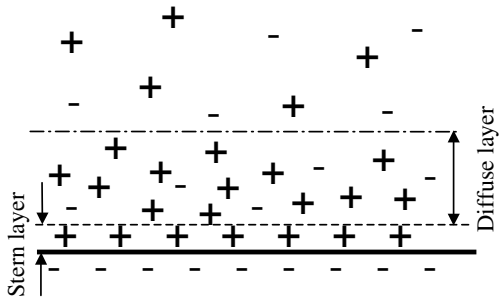

Fig. 1. The schematic of the electric double layer showing the Stern layer and diffuse layer.

The Stern layer is a thin region in which counterions are adsorbed onto the charged surface. Although ions in the Stern layer are fixed in place, ions in the diffuse layer are free to migrate. The plane between the Stern layer and diffuse layer is called the "shear plane." The potential at this plane is called the "zeta potential," or "ζ." Under an applied electric field, the diffuse layer positive ions move in the direction of the field, causing the ion drag on the liquid. The liquid motion in the diffuse layer is translated to the rest of the channel via viscous forces.

The conservation of mass, momentum, and energy equations can be expressed as follows for the flow of an incompressible, Newtonian, isotropic fluid in the presence of an external electric field

$$\frac{\partial u_i}{\partial x_i} = 0 \tag{4}$$

$$\rho\left(\frac{\partial u_i}{\partial t} + u_j\frac{\partial u_i}{\partial x_j}\right) = -\frac{\partial P}{\partial x_i} + \frac{\partial}{\partial x_i}\left[\mu\left(\frac{\partial u_i}{\partial x_j} + \frac{\partial u_j}{\partial x_i}\right)\right] + \rho_E E_i \tag{5}$$

$$\rho C_v\left(\frac{\partial T}{\partial t} + u_i\frac{\partial T}{\partial x_i}\right) = \frac{\partial}{\partial x_i}\left(k\frac{\partial T}{\partial x_i}\right) + \rho_E E_i u_i \tag{6}$$

where μ is the viscosity; ρ_E is the electric charge density; E is the external electric field; C_v is the specific heat at constant volume; and k is the thermal conductivity. The term $\rho_E E_i$ in momentum equation is the Lorentz body force, and the term $\rho_E E_i u_i$ in the energy equation is the corresponding work term.

For one-dimensional, fully developed electro-osmotic flow, Eq. (5) reduces to

$$0 = -\frac{dP}{dx} + \mu\frac{\partial^2 u}{\partial y^2} + \rho_E E_x = -\frac{dP}{dx} + \mu\frac{\partial^2 u}{\partial y^2} - \varepsilon\frac{\partial^2 \phi}{\partial y^2}E_x \tag{7}$$

where ε is the permittivity and ϕ is the electric potential, and a constitutive equation has been applied.

The distinction between electroosmotic and pressure-driven flow profiles is seen in Fig. 2. In the case of pressure driven flows, a pressure gradient (<1 bar/cm) is maintained along a channel, causing flow to occur in an opposing direction. This is a classical type of flow used in many engineering applications at the macro level and is known as "Poiseuille flow." It may be modeled using the Navier–Stokes equations. At low Reynolds number, the flow is

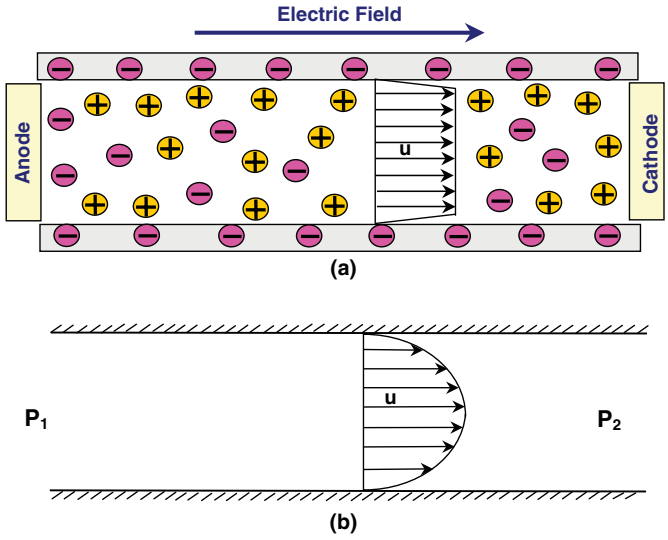

Fig. 2. The schematic of velocity profiles for (a) electro-osmotic flow (b) pressure-driven flow.

uniaxial along the principal axis of the channel, and the speed of the flow varies in a parabolic manner over the cross-section of the channel. This variation of speed over the cross-section leads to rapid dispersion of bands of solute in the flow as the volume of fluid occupied by the solute is stretched along the flow direction, and the portion of the volume near the center of the channel outpaces the portion near the walls. This is a main disadvantage as the increased dispersion degrades the performance of electro-kinetic separations by impacting the resolution of closely eluted peaks. It also affects the ability to control the movement of discrete samples within a microfluidic device. Pressure-driven flow devices also often contain moving parts, which are not desirable in applications involving bioanalysis. Flows of this type cannot be used in applications involving separation of mixtures. Some of the advantages of pressure-driven flows are that they can be applied to any type of solvent and they are insensitive to surface contaminations. Pressure gradients can be generated by low voltage, gravity, osmosis, etc., providing a wide range of flow speeds (<100 cm/s).

2.2. Materials

The development of materials for chemical and biological analysis systems has gained enormous interest recently. Perhaps the most striking example of these improvements is provided by the great success of capillary electrophoresis in speeding up the sequencing of the first human genome. In the selection of appropriate material for microfluidic devices, material properties need to be carefully evaluated. Some of the important material properties include machinability, molecular adsorption, and optical properties. Glass, silicon, and plastics have been used as microchannel materials to date. While silicon and glass dominated the early years, a trend toward polymers as substrate material has been observed. Use of poly-dimethylsiloxane (PDMS); poly-methyl methacrylate (PMMA); poly-trifluoroethylene (PTFE), commonly known as "Teflon"; poly-methyl methacrylate (acrylic); and quartz became common in the recent past [8,12,13]. Becker and Locascio [14] compared material properties and fabrication of six polymer substrates, namely methyl-methacrylate, poly-carbonate, poly-ester, poly-styrene, poly-vinylchloride, and silicones. A study on microchannels using metals, especially stainless steel and aluminum, was also carried out in the past to investigate friction and pressure drop characteristics [15,16]. These investigations are more in line with applications such as microheat exchangers. The current trend for biomedical applications strongly points towards use of polymer-based substrates. In parallel to the development of microfluidic devices, microfabrication techniques have also evolved significantly. Some of the important fabrication techniques include lithography (soft and photolithography), lamination, injection molding, hot embossing, micromachining with laser, and electrochemical or ultrasonic technologies [5,14,17,18].

2.3. Microchannels cross-sections and entrance effects

Several investigators used different cross-sections such as rectangular, circular, trapezoidal, triangular, and elliptical to understand the flow behavior in microchannels. Rectangular and trapezoidal cross-sections have been extensively studied for a wide range of applications, mainly due to practical considerations such as fabrication techniques, cost, ease of manufacturing, etc. Researchers employed rectangular cross-sections for studying different physical phenomena such as friction and pressure drop [16,19–22], electro-viscous effects [23], velocity measurements [24–26], flow control [4,13,27], and flow visualization [28]. Some notable studies using trapezoidal cross-sections are by Ross et al. [8], Takuto et al. [29], Liu et al. [30], Wu and Cheng [31], and Barker et al. [12]. Ross et al. [8] investigated sample dispersion in electro-osmotic flows in plastic microchannels. Frictional and pressure drop characteristics were studied by several researchers [29–31]. Studies on control of flow direction using polyelectrolyte multilayers were carried out by Barker et al. [12]. The use of circular cross-sections is mainly limited to heat transfer equipment such as microheat exchangers.

Even though a tremendous effort in microfluidics research is currently underway, there is little work done to study the entry flow in microchannels. Researchers generally assumed microchannel flows as laminar and fully developed ignoring entrance effects. However, in the entry region, velocity distribution and skin friction show significant variations in the stream-wise direction, which could influence separation efficiency in processes such as electrophoresis. Yang et al. [32] numerically simulated the flow physics in the entry region of an electro-osmotic flow. Their results indicated greater entrance length effects of the electro-osmotic flow as well as higher skin friction coefficient

than for classical pressure driven flow. Campbell and Kandlikar [33] studied the effects of entrance conditions on microchannel and minichannel pressure gradient and laminar to turbulent transition in a circular pipe. The observed, fully developed, friction factor times Reynolds number (which is constant for laminar flows in large diameter tubes) had an increasing value with increasing Reynolds numbers, even for low Reynolds numbers, for both tubes.

Unlike previous researchers, Kohl et al. [1] did not find any indication of early laminar-to-turbulent transition. The previous findings on early transitions might be connected to unaccounted effects such as entrance geometry and energy dissipation.

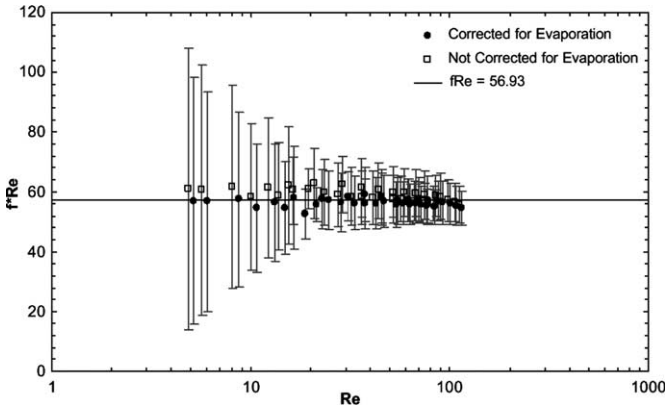

Fig. 3. Friction factor data showing the effect of evaporation. Working fluid: water; microchannel type: rectangular cross-section silicon microchannel. Reprinted from Kohl et al. [1] with kind permission of Elsevier.

2.4. Pressure drop and friction

Characterization of frictional pressure drop for fluid flows through microchannels is a subject of continuous debate since experimental results are often inconsistent and contradictory. In the last two decades, a number of papers have reported pressure drop data on laminar flow of liquids and gases inside microchannels [16,20,22,29,31]. Recently, discrepancies among the work of many researchers have been summarized in a review paper by Koo and Kleinstreuer [34]. Peng and Peterson [15] and Peng et al. [19] observed either increase or decrease of friction factor/pressure drop compared to conventional theory, and they attributed this to an early onset of laminar to turbulent flow transition. Mala and Li [35], Papautsky et al. [20], and Ren et al. [23] assumed the deviation would originate from surface phenomena. Most of their results indicate that the friction factor/pressure gradient would increase due to the effects of surface phenomena. Xu et al. [22] and Judy et al. [16] insisted that the friction factor/pressure gradient results are the same as the values predicted by conventional theory. They claimed that the deviations, which other researchers had observed, might have originated from measurement errors of channel size, experimental uncertainties, and overlooked entrance effects. The use of the Navier–Stokes equations appears to be appropriate for microchannel flows of liquids as long as the hydraulic diameter of system is greater than 0.1 μm for conduits filled with Newtonian fluids such as water under the standard conditions [34]. However, Navier–Stokes must be modified or augmented with auxiliary equations whenever it is required to deal with non-Newtonian fluids and when surface phenomena, such as near-wall forces and relative roughness, becomes more and more important as the microchannel size becomes smaller. In a recent publication, Kohl et al. [1] measured pressure drop in microchannels in an attempt to determine the sources of often conflicting results previously reported in the literature. They integrated tap lines and pressure sensing membranes into the microchannel system, which allowed them to measure pressure directly inside the microchannel. They pointed out that this technique obviated the need of making of assumptions completely while measuring pressure. According to Kohl et al. [1], indirect means of measuring pressure inside microchannels resulted in under- or over-estimating pressure drop. They also indicated evaporation phenomenon is important in measuring mass flow rate in microchannels, and the unaccounted evaporation rates might lead to errors as much as 10% (see Fig. 3). Hetsroni et al. [2] highlighted the significant effect of surface roughness on the pressure drop in microchannels. They proposed a roughness-viscosity model to take into account the influence of surface roughness.

2.5. Flow control in microchannels

A diversity of fluid properties and microfluidic device applications translates into a wide variety of requirements in microscale flow control. Some examples of fluid control in microchannels include the positioning streams within the cross-section of the channel for the precise delivery of reagents, the mixing of solutions required for chemical reactions, and the transportation of small volumes of solution for high throughput syntheses and analyses. Numerous techniques such as patterned surface charge, patterned topography, three-dimensional channels, magnetohydrodynamics, patterned wettibility, peristalsis, and patterned electrodes have been tested to control electro- osmotic (EO) and pressure-driven flows. Such patterned surface charges (EO) have been used for manipulating flows in microchannels. While techniques like patterned surface charge and patterned electrodes can only be useful to control electro-osmotic flows, others such as three-dimensional channels, patterned wettibility, and peristalsis can be used to control pressure driven flow. Patterned topography can be applied to both types of flows. All of these techniques have been used as various mechanisms to control dispersion, mixing, pumping, etc.

Stroock and Whitesides [4] reviewed two procedures for controlling the flow of fluids in microchannels. The first procedure involves patterning the density of charge on

the inner surfaces of a channel. These patterns generate recirculating electro-osmotic flows in the presence of a steady electric field. The second procedure involves patterning topography on an inner surface of a channel. These patterns generate recirculation in the cross-section of steady, pressure driven flows. The generation of recirculation zones in microflows has applications to mixing as well as controlling dispersion. Active and passive microflow control has been demonstrated by Stoeber et al. [27], using gel formation by dilute aqueous solutions of poloxamers at elevated temperatures. In both cases, gel formation, which effectively blocks the flow, is the control mechanism. In case of active control, gel formation is caused by integrated resistive heaters for localized heating, and in case of passive control, viscous heating in high shear rate flows leads to automatic gel formation in a microchannel. Barker et al. [12] demonstrated the use of polyelectrolyte multilayers (PEMs) to alter the surface charge to control the flow direction in polystyrene and acrylic microfluidic devices. They could generate complex flow patterning and achieve even flow in opposite directions within a single channel. Sui and Schlenoff [36] demonstrated control of electro-osmotic flow in microchannels with pH-responsive PEMs. Ismagilov et al. [13] published a method to control fluid flow through tangentially connected microchannels by means of an elastomeric microfluidic switch in two ways. In the first approach, flow control is achieved by changing the aspect ratio of microchannels through application of external pressure. In the second approach, the flow direction is controlled by injecting additional streams of fluid into the channel, which changes the lateral position of the stream within the channel on which flow direction depends. Goettsche et al. [37] developed an active control method where they used a piezoactuated micromachined silicone microvalve to control flow rate with a high degree of precision for drug delivery applications. Centrifugal platforms have been considered as elegant means to transport fluids in these labs-on-a-chip. Ducree et al. [38] investigated how the pseudo-Coriolis force can be employed for the hydrodynamic control of flow through straight and radial microchannels of a rectangular cross-section on a rotating disk. Based on this effect, a novel flow switch has been realized. Polson and Hayes [39] demonstrated the development of external voltage control of electro-osmotic flow for microfabricated fluidic microdevices. The external voltage flow control technique requires no permanent changes in surface structure nor altered buffers, which is an advantage in many applications where altering structures or buffers are not acceptable. Hasselbrink et al. [40] developed a non-stick polymer formulation for creating moving parts inside of microfluidic channels. They applied the technique to create a piston-based device that overcomes several microfluidic flow control challenges. The major advantage of this technique is that moving parts can be made without the limitations and difficulties imposed by the need for sacrificial layers or mechanical assembly.

2.6. Mixing in microchannels

Rapid mixing is an integral part of many applications that involve microfluidic systems. Desired mixing is essential in lab-on-chip devices, drug delivery, and systems that carry out complex chemical synthesis. The literature contains a number of methods and devices designed to enhance mixing on the microscale. Active mixing produces excellent mixing; however, the means of achieving mixing could involve moving parts which are difficult to fabricate and integrate into the microfluidic systems. Passive mixing utilizes no external energy input and depends mainly on the mechanism used to generate fluid flow through the microchannels; consequently, only limited mixing can be achieved. Flow mixing can be thought of as "flow control" since mixing to the desired degree can be viewed as one of the requirements of flow control. In this context, procedures involve patterning the density of charge as well as patterning topography on an inner surface of a channel can be used for mixing purposes as both techniques produce recirculation zones in addition to controlling the dispersion [4,41]. The former method produces recirculation zones in the presence of a steady electric field, and in the latter case, recirculation zones are produced in pressure driven flows. Liu et al. [30] presented a microchannel design as a method to produce passive mixing based on the twisted pipe. They used serpentine microchannel design with a "C-shaped" repeating unit to enhance mixing, which is achieved through the chaotic advection. Vijayendran et al. [42] compared the mixing capabilities of a straight and serpentine microchannel in a surface-based biosensor. They observed a slight improvement in three-dimensional serpentine geometry compared to a simpler straight channel. He et al. [43] designed and fabricated a 100 pL mixer. In this design, the channels parallel to the flow were narrow, whereas a larger channel ran back and forth across the set of parallel channels at an angle of 45°. Simulations were also performed to describe the mixing within this system. Oddy et al. [44] developed an electro-kinetic process to rapidly stir micro- and nanoliter volume solutions. Mixing is caused by flow instability, which is observed in sinusoidally oscillating, electro-osmotic channel flows. Lee et al. [45] achieved mixing of fluid and particles through chaotic mixing. The chaotic mixing process is achieved by inducing folding and stretching of material lines, which are generated by either superimposing unsteady pressure perturbations or time-dependent dielectrophoretic forces to a mean stream.

2.7. Joule heating and viscous dissipation effects

Pumping the fluid in a microchannel by means of electroosmosis requires the application of a high external electric field along the channel. In this case, the Joule heating arises from two effects: one is due to the convection electric current, and the other one is due to the conduction electric current. Since the electric charge density is only active

within the effective EDL, the contribution of the convection electric current is not dominant in the Joule heating compared to the conduction electric current. The Joule heating effect may become significant, depending on the volume of the channel. In some cases, the contribution of the Joule heating term to the thermal energy transport equation might be major over the entire volume. Horiuchi and Dutta [46] reported that the Joule heating effect is significant over the entire volume if the channel thickness is higher than 20 μm. To diminish the effect of Joule heating, Lim et al. [47] proposed improving the heat dissipation by means of finned channel geometry. The optimum geometry corresponding to the lowest temperature rise was evaluated for glass microchannels with large cross-sections (500 μm × 275 μm) in this study. Tang et al. [48] compared the transient temperature fields of liquid solution in glass and PMMA polymer-based microchannels by including the Joule heating effect in the coupled Poisson–Boltzman (P–B) equation, the modified Navier–Stokes equation (N–S), energy equation, and the mass species transport equation. The analyses took into consideration the temperature dependent thermophysical properties of NaCl solution. Their results demonstrated that the Joule heating effect is significant in the case of poor thermal conductivity of the channel wall (i.e., PMMA wall). Chen and Santiago [49] developed an electroosmotic (EO) pump that can pump the fluid against up to 1.5 atm counter pressure. They indicated that the Joule heating effect sets the upper limit for the operating voltage of this type of pump. Since the major constituent of the power consumption of EO pump was devoted to the Joule heating, the thermodynamic efficiency of the EO pump was quite low.

The degrading effect of the Joule heating in system efficiency was observed not only in EO pumps but also in capillary electrophoresis (CE) systems that are used to separate biological molecules. The indication of the loss of separation efficiency in capillary electrophoresis (CE) systems led Swinney and Bornhop [50] to develop a non-invasive thermometry for the direct measurement of the extent of Joule heating in CE systems. This study showed that even relatively low electrical field strengths (475 V/cm) resulted in an increase of 2.81 °C temperature above ambient.

For an EDL much smaller than the channel dimensions, the energy generation due to the Joule heating effect is uniform through the microchannel cross-section. However, the energy generation due to the viscous dissipation is not uniformly distributed over the cross-section. Koo and Kleinstreuer [51] investigated the effect of viscous dissipation in microtubes and microchannels using three working fluids: water, methanol, and iso-propanol. Their numerical analysis for pressure-driven flow revealed that viscous dissipation effects might be significant for fluids with low specific heat capacities and high viscosities. They also indicated that high aspect ratio microchannels lead to higher viscous dissipation. Maynes and Webb [52] analyzed the effect of viscous dissipation for electro-osmotic flow. Their analysis assumed constant fluid properties for viscosity, electrical and thermal conductivity. A further analysis is needed for electro-osmotic flow, which takes into account the temperature dependent thermophysical properties of working fluid.

3. Velocimetry techniques for microchannel flows

As the interest in the design of microfluidic devices grows, understanding the characteristics of a flow at the microscale through accurate measurement and visualization techniques become increasingly important. Some of the widely used measurement techniques in macroscopic flow systems such as particle image velocimetry (PIV), laser Doppler velocimetry (LDV), and scalar image velocimetry (SIV) were modified for micron-resolution measurements. New experimental techniques, specifically developed for microfluidics, also emerged. This section will only present information on the PIV and dye-based techniques.

3.1. PIV measurements

PIV is a well known and commonly used technique in the macroscale flow diagnostic. The application of this technique to the microscale required resolving additional issues related to miniaturized systems such as using compatible particle size to the size of microfluidic system. Paul et al. [53] applied the SIV to visualize both pressure driven and electro-osmotic flow. Santiago et al. [54] and Meinhart et al. [24] successfully implemented micro-PIV in pressure driven microflow systems and measured velocity fields on the order of 1 μm spatial resolution. Devasenathipathy and Santiago [25] obtained electro-osmotic flow fields at a microchannel intersection using the micro-PIV in conjunction with the particle tracking velocimetry (PTV). Meinhart et al. [55] suggested the volume illumination of micro-PIV system instead of illuminating via a two-dimensional sheet of light when optical access is limited to only one direction of the microchannel. The application of volume illumination for micro-PIV might be desirable for silicon-based microchannels, which are fabricated by bonding the glass wafer onto the silicon structure. However, this alternative micro-PIV technique generates a high background noise due to receiving signals from out of focus seed particles. Reducing concentration of seed particles improves the signal-to-noise ratio in the expense of reducing the spatial resolution of measurements.

In general, quantitative PIV measurements require careful selection of size and concentration of seed particles since the flow and the velocity information of the flow is extracted indirectly by observing the displacement of the particles. The seed particles should be distributed uniformly throughout the fluid, exhibit neutral buoyancy, and have no other effect on the fluid or flow properties for accurate measurements. The selection of seed particles is a challenging task for quantitative micro-PIV measurements. The seed particles must be small enough to track the flow faithfully, but at the same time, they must be large

enough to scatter sufficient light. The size of seed particles must be compatible with the size of the flow system, but seed particles must also be in appropriate size to reduce the effect of Brownian motion. Olsen and Adrian [56] examined the effects of Brownian motion on the depth correlation of PIV images.

3.2. Velocimetry techniques using dye tracers

Dye-based microflow visualization techniques, which are alternatives to particle tracking techniques, employ a dilute solution of highly fluorescent molecules as a flow tracer. The caged-fluorescence imaging technique extracts transport properties of microfluidic systems by photoactivating a small amount of caged dye [8,53,57–59]. The initially transparent caged dye is converted to the uncaged dye (free fluorescent dye) by exposing it to ultraviolet (UV) light. The second laser excitation allows the uncaged dye molecules to fluoresce, and Laser Induced Fluorescence images are acquired at a sequence of delay times to track the transport of uncaged dye. The caged-fluorescence imaging technique requires a microfluidic system that is transparent to UV light. Another dye based technique, the photobleached-fluorescence technique, is based on the photobleaching effect, which is defined as photodecomposition of fluorescent molecules upon a brief exposure to a high intensity light or a long exposure to a lower intensity light. When fluorescent molecules in a region of the flow field are photobleached, that particular region appears as a dark region in a bright fluorescent background. Mosier et al. [28] visualized the electro-kinetic flow in a curved microchannel by tracing fluorophore dye molecules in the flow via the photobleached-fluorescence technique. This technique is suitable both for polymer and glass microchannel systems that are transparent to visible light.

Mosier et al. [28] indicated that the caged-fluorescence imaging provides better signal-to-noise ratio compared to the photobleached-fluorescence imaging. The charging characteristics of uncaged dye may alter the results of caged-fluorescence imaging due to the repelling of charged dye molecules from negatively charged channel walls in elektrokinetic flow [60]. Ross and Locascio [61] indicated that the adsorption of caged dye at the polymer microchannel walls effects the caged-fluorescence results, especially for elektrokinetic flow. They compared EOF mobilities of microchannel systems made of four different materials: PMMA, PDMS, PC, and fused-silica. The investigation revealed that the EOF mobility increases for polymer microchannels when CMNB-caged fluorescence dye is added to the carbonate buffer. No significant effect was observed for the fused-silica microchannel. Therefore, this technique might be limited to applications in fused-silica channels.

Techniques that measure the average flow velocity by tracking the emitted radiation from the heated liquid in microchannels are also available. Chung et al. [26] measured the velocity of the maximum radiative intensity point (V_{MRIP}) by using the infrared thermal velocimetry. The infrared thermal velocimetry is based on extracting the velocity information from the thermal image of moving fluid flowing in a silicon microchannel. This technique is not suitable to obtain a velocity profile and can be used only when the microchannel is made of silicon.

Park et al. [62] integrated resistance temperature detectors into a rectangular straight microchannel to measure the temperature distribution of the fluid in the microchannel. The pressure drop and micro-PIV measurements were conducted to investigate the effect of varying channel wall temperature on the flow resistance and velocity profile. The authors indicated that the variation of physical properties of the fluid along the microchannel, caused by varying channel wall temperature, have significant effect on the flow resistance. In addition to this, the velocity measurements revealed that the maximum fluid velocity along the channel increases with the increasing channel wall temperature. These results show that when a microchannel system is exposed to thermal effects, the temperature-dependent thermophysical properties of the fluid should be taken into consideration.

Table 1
Summary of potential research areas related to microfluidic systems

General area and related studies	Potential research areas
1. Characteristics of flow in microchannels	
(a) Microchannel cross-sections [8,19]	Triangular, elliptical, and non-uniform cross-sections
(b) Entrance effects [33]	Analysis for smaller channels. Entrance effects on flow control
(c) Friction factor and pressure drop [16,20,34]	Contradictions among various investigations and establishing some benchmark studies
(d) Surface roughness [63]	Effect of surface heterogeneity and defects
(e) Joule heating [22,46,49]	Temperature effects on electro-osmotic flow profiles
(f) Viscous dissipation [51,52]	Viscous dissipation effects in fluids other than water
(g) Materials [5,14,17]	Fabrication methods, cost reduction criterion. Use of flexible materials
2. Flow control in microchannels	
(a) Flow control and separation [4,37]	Leaks in microfluidic valves. Low separation efficiencies
(b) Flow mixing [4,41]	Enhancing mixing at micro scales, modeling of active mixtures
3. Experimental techniques for microchannel flows	
(a) Micro-PIV [25,55]	Accounting for motion of seed particles due to electrophoretic and electro-osmotic forces
(b) Caged-fluorescence imaging [59,61]	Spectral, charging, and separation properties of caged dye candidates; determination of optimum caged dye concentration for cost effective application

4. Future directions in microfluidics research

The research in microfluidics has attracted attention in the recent past due to the possibility of commercialization of technology, especially in the area of biotechnology. Currently, tremendous effort is underway and a vast amount of literature is available for an interested researcher. Despite the fact that a large amount of information is available, it is surprising to see that basic information on microfluidics, such as types of flows and the associated governing equations, are not readily available. In this context, the authors attempted to compile information on basic microfluidic theory and the current state of research. Table 1 gives some notable research studies as well as topics that need further investigation.

5. Conclusions

Based on an extensive literature review, the authors conclude that there are many possible areas of research in the field of microfluidics. For example, experimental results on pressure drop and friction factor measurements reported in the literature are mostly inconsistent and contradictory. Several papers on microscale flow indicated early transition from laminar to turbulent flow and deviations between the predictions of conventional theory and experimental results on pressure drop and friction factor. The reported experiments in the literature include a variety of fluid types, microchannel cross-section shapes and sizes, different Reynolds numbers, and channel materials with a range of surface roughness. Kohl et al. [1] and Hetsroni et al. [2] suggested the following possible reasons for the inconsistent results encountered in the literature: experimental uncertainties in the measurements of channel dimensions and flow rates (especially neglecting the effect of evaporation during the flow rate measurements); differences in surface roughness; unaccounted Joule heating and viscous dissipation effects; unaccounted electro-viscous effects for pressure-driven flows; unaccounted entrance and exit effects. Benchmark studies, which carefully examine pressure drop, friction factor, and entrance and exit effects in microchannels are strongly needed.

The use of fluorescent dye as flow tracers is a promising approach for extracting the fluid dynamics properties of microfluidic systems without disturbing the flow. However, it appears that more work is needed to understand some important properties of dye candidates such as spectral, charging, and separation properties. Researchers should also take into account the cost of each dye candidate for caged-fluorescence imaging since caged dyes can be used only once due to the irreversible nature of the uncaging event.

In general, most of the experimental work is done involving Newtonian fluids, mostly using either water or water-based solutions. Lab-on-a-chip type applications definitely warrant the characterization of bio-fluids such as human blood, which is a non-Newtonian fluid. Understanding the behavior of non-Newtonian fluids at microscale is indeed an important step towards realization of micro assay devices. Another significant research area that needs extensive investigation is that of the flow control. Flow control is still not fully understood at the microscale level, and existing techniques must be thoroughly investigated and improved significantly.

Acknowledgement

We acknowledge Dr. A. Sidney Roberts, Jr. for reading the manuscript and for his critical comments.

References

[1] M.J. Kohl, S.I. Abdel-Khalik, S.M. Jeter, D.L. Sadowski, An experimental investigation of microchannel flow with internal pressure measurements, Int. J. Heat Mass Transfer 48 (2005) 1518–1533.
[2] G. Hetsroni, A. Mosyak, E. Pogrebnyak, L.P. Yarin, Fluid flow in micro-channels, Int. J. Heat Mass Transfer 48 (2005) 1982–1998.
[3] C.-M. Ho, Y.-C. Tai, Micro-electro-mechanical systems (MEMS) and fluid flows, Ann. Rev. Fluid Mech. 30 (1998) 579–612.
[4] A.D. Stroock, G.M. Whitesides, Controlling flows in microchannels with patterned surface charge and topography, Accounts Chem. Res. 36 (2003) 597–604.
[5] B.H. Weigl, R.L. Bardell, C.R. Cabrera, Lab-on-a-chip for drug development, Adv. Drug Delivery Rev. 55 (2003) 349–377.
[6] D. Sinton, C. Escobedo-Canseco, L. Ren, D. Li, Direct and indirect electroosmotic flow velocity measurements in microchannels, J. Colloid Interface Sci. 254 (2002) 1–6.
[7] A.T. Conlisk, J. McFerran, Z. Zheng, D. Hansford, Mass transfer and flow in electrically charged micro- and nanochannels, Anal. Chem. 74 (2002) 2139–2150.
[8] D. Ross, T.J. Johnson, L.E. Locascio, Imaging of electroosmotic flow in plastic microchannels, Anal. Chem. 73 (2001) 2509–2515.
[9] D. Burgreen, F.R. Nakache, Electrokinetic flow in ultrafine capillary slits, J. Phys. Chem. 68 (1964) 1084–1091.
[10] R.F. Probstein, Physicochemical Hydrodynamics, second ed., Wiley, New York, 1994, pp. 195–200.
[11] S. Levine, J.R. Marriott, G. Neale, N. Epstein, Theory of electrokinetic flow in fine cylindrical capillaries at high zeta-potentials, J. Colloid Interface Sci. 52 (1) (1974) 136–149.
[12] S.L.R. Barker, D. Ross, M.J. Tarlov, M. Gaitan, L.E. Locascio, Control of flow direction in microfluidic devices with polyelectrolyte multilayers, Anal. Chem. 72 (2000) 5925–5929.
[13] R.F. Ismagilov, D. Rosmarin, P.J.A. Kenis, D.T. Chiu, W. Zhang, H.A. Stone, G.M. Whitesides, Pressure-driven laminar flow in tangential microchannels: an elastomeric microfluidic switch, Anal. Chem. 73 (2001) 4682–4687.
[14] H. Becker, L.E. Locascio, Polymer microfluidic devices, Talanta 56 (2002) 267–287.
[15] X.F. Peng, G.P. Peterson, Convective heat transfer and flow friction for water flow in microchannel structures, Int. J. Heat Mass Transfer 39 (1996) 2599–2608.
[16] J. Judy, D. Maynes, B.W. Webb, Characterization of frictional pressure drop for liquid flows through microchannels, Int. J. Heat Mass Transfer 45 (2002) 3477–3489.
[17] T. Chovan, A. Guttman, Microfabricated devices in biotechnology and biochemical processing, TRENDS Biotechnol. 20 (3) (2002) 116–122.
[18] W. Ehrfeld, Electrochemistry and microsystems, Electrochim. Acta 48 (2003) 2857–2868.

[19] X.F. Peng, G.P. Peterson, B.X. Wang, Frictional flow characteristics of water flowing through rectangular microchannels, Exp. Heat Transfer 7 (1994) 249–264.
[20] I. Papautsky, B.K. Gale, S. Mohanty, T.A. Ameel, A.B. Frazier, Effects of rectangular microchannel aspect ratio on laminar friction constant, in: C.H. Ahn (Ed.), Proceedings of the SPIE Microfluidic Devices and Systems, Santa Clara, CA, vol. 3877, 1999, pp. 147–158.
[21] W.Y. Lee, M. Wong, Y. Zohar, Pressure loss in constriction microchannels, J. Microelectromech. Syst. 11 (3) (2002) 236–244.
[22] B. Xu, K.T. Ooi, N.T. Wong, W.K. Choi, Experimental investigation of flow friction for liquid flow in microchannels, Int. Commun. Heat Mass Transfer 27 (8) (2000) 1165–1176.
[23] L. Ren, W. Qu, D. Li, Interfacial electrokinetic effects on liquid flow in microchannels, Int. J. Heat Mass Transfer 44 (2001) 3125–3134.
[24] C.D. Meinhart, S.T. Wereley, J.G. Santiago, PIV measurements of a microchannel flow, Exp. Fluids 27 (1999) 414–419.
[25] S. Devasenathipathy, J.G. Santiago, Particle tracking techniques for electrokinetic microchannel flows, Anal. Chem. 74 (2002) 3704–3713.
[26] J. Chung, C.P. Grigoropoulos, R. Greif, Infrared thermal velocimetry for non-intrusive flow measurements in silicon microfluidic devices, Rev. Scientific Instrum. 74 (5) (2003) 2911–2917.
[27] B. Stoeber, D. Liepmann, S.J. Muller, Microflow control using thermally responsive triblock copolymers, in: Proceedings of the Seventh International Symposium on Micro Total Analysis Systems, Squaw Valley, CA, 2003, pp. 183–186.
[28] B.P. Mosier, J.I. Molho, J.G. Santiago, Photobleached-fluorescence imaging of microflows, Exp. Fluids 33 (2002) 545–554.
[29] A. Takuto, K.M. Soo, I. Hiroshi, S. Kenjiro, An experimental investigation of gaseous flow characteristics in microchannels, in: Proceedings of the International Conference on Heat Transfer and Transport Phenomena in Microscale, Banff, Canada, 2000, pp. 155–161.
[30] R.H. Liu, M.A. Stremler, K.V. Sharp, M.G. Oslen, J.G. Santiago, R.J. Adrian, H. Aref, D.J. Beebe, Passive mixing in a three-dimensional serpentine microchannel, J. Microelectromech. Syst. 9 (2) (2000) 190–197.
[31] H.Y. Wu, P. Cheng, Friction factors in smooth trapezoidal silicon microchannels with different aspect ratios, Int. J. Heat Mass Transfer 46 (2003) 2519–2525.
[32] R.J. Yang, L.M. Fu, C.C. Hwang, Electroosmotic entry flow in a microchannel, J. Colloid Interface Sci. 244 (2001) 173–179.
[33] L.A. Campbell, S.G. Kandlikar, Effect of entrance condition on frictional losses and transition to turbulence in minichannel flows, in: Proceedings of the Second International Conference on Microchannels and Minichannels, Rochester, NY, 2004, ICMM, pp. 2004–2339.
[34] J. Koo, C. Kleinstreuer, Liquid flow in microchannels: experimental observations and computational analyses of microfluidics effects, J. Micromech. Microeng. 13 (2003) 568–579.
[35] G.M. Mala, D. Li, Flow characteristics of water in microtubes, Int. J. Heat Mass Transfer 20 (1999) 142–148.
[36] Z. Sui, J.B. Schlenoff, Controlling electroosmotic flow in microchannels with pH-responsive polyelectrolyte multilayers, Langmuir 19 (2003) 7829–7831.
[37] T. Goettsche, J. Kohnle, M. Willmann, H. Ernst, S. Messner, R. Steger, M. Storz, W. Lang, R. Zengerle, H. Sandmaier, Novel approaches to microfluidic components in high-end medical applications, in: Proceedings of the 12th International Conference on Solid State Sensors, Actuators and Microsystems, Boston, MA, 2003, pp. 623–626.
[38] J. Ducree, T. Brenner, T. Glatzel, R. Zengerle, Coriolis-induced switching and mixing of laminar flows in rotating microchannels, in: Proceeding of the 2nd VDE World Micro-technologies Congress, Munich, Germany, 2003, pp. 397–404.
[39] N. Polson, M.A. Hayes, Electroosmotic flow control of fluids on a capillary electrophoresis microdevice using an applied external voltage, Anal. Chem. 72 (2000) 1088–1092.
[40] E.F. Hasselbrink Jr., T.J. Shepodd, J.E. Rehm, High-pressure microfluidic control in lab-on-a-chip devices using mobile polymer monoliths, Anal. Chem. 74 (2002) 4913–4918.
[41] A.D. Stroock, S.K. Dertinger, G.M. Whitesides, A. Ajdari, Patterning flows using grooved surfaces, Anal. Chem. 74 (2003) 5306–5312.
[42] R.A. Vijayendran, K.M. Motsegood, D.J. Beebe, D.E. Leckband, Evaluation of a three-dimensional micromixer in a surface-based biosensor, Langmuir 19 (2003) 1824–1828.
[43] B. He, B.J. Burke, X. Zhang, R. Zhang, E. Fred, F.E. Regnier, A picoliter-volume mixer for microfluidic analytical systems, Anal. Chem. 73 (2001) 1942–1947.
[44] M.H. Oddy, J.G. Santiago, J.C. Mikkelsen, Electrokinetic instability micromixing, Anal. Chem. 73 (2001) 5822–5832.
[45] Y.K. Lee, J. Deval, P. Tabeling, C.H. Ho, Chaotic mixing in electrokinetically and pressure driven micro flows, in: Proceedings of the 14th IEEE Workshop on MEMS, Interlaken, Switzerland, 2001, pp. 483–486.
[46] K. Horiuchi, P. Dutta, Joule heating effects in electroosmotically driven microchannel flows, Int. J. Heat Mass Transfer 47 (2004) 3085–3095.
[47] D.S.W. Lim, J.S. Kuo, D.T. Chiu, Parametric investigation on the effect of channel topologies on electrophoretic separations, J. Chromatogr. A 1027 (2004) 237–244.
[48] G.Y. Tang, C. Yang, C.K. Chai, H.Q. Gong, Numerical analysis of the thermal effect on electroosmotic flow, Anal. Chimica Acta 507 (2004) 27–37.
[49] C.H. Chen, G. Santiago, A planar electroosmotic micropump, J. Microelectromech. Syst. 11 (6) (2002) 672–683.
[50] K. Swinney, D.J. Bornhop, Quantification and evaluation of Joule heating in on-chip capillary electrophoresis, Electrophoresis 23 (2002) 613–620.
[51] J. Koo, C. Kleinstreuer, Viscous dissipation effects in microtubes and microchannels, Int. J. Heat Mass Transfer 47 (2004) 3159–3169.
[52] D. Maynes, B.W. Webb, The effect of viscous dissipation in thermally fully-developed electro-osmotic heat transfer in microchannels, Int. J. Heat Mass Transfer 47 (2004) 987–999.
[53] P.H. Paul, M.G. Garguilo, D.J. Rakestraw, Imaging of pressure- and electrokinetically driven flows through open capillaries, Anal. Chem. 70 (1998) 2459–2467.
[54] J.G. Santiago, S.T. Wereley, C.D. Meinhart, D.J. Beebe, R.J. Adrian, A particle image velocimetry system for microfluidics, Exp. Fluids 25 (1998) 316–319.
[55] C.D. Meinhart, S.T. Wereley, M.H.B. Gray, Volume illumination for two-dimensional particle image velocimetry, Measur. Sci. Technol. 11 (2000) 809–814.
[56] M.G. Olsen, R.J. Adrian, Brownian motion and correlation in particle image velocimetry, Optics Laser Technol. 32 (2000) 621–627.
[57] W.R. Lempert, K. Magee, P. Ronney, K.R. Gee, R.P. Haugland, Flow tagging velocimetry in incompressible flow using photo-activated non-intrusive tracking of molecular motion (PHANTOMM), Exp. Fluids 18 (1995) 249–257.
[58] A.E. Herr, J.I. Molho, J.G. Santiago, M.G. Mungal, T.W. Kenny, Electroosmotic capillary flow with nonuniform zeta potential, Anal. Chem. 72 (2000) 1053–1057.
[59] D. Sinton, D. Li, Microfluidic velocimetry with near-wall resolution, Int. J. Thermal Sci. 42 (2003) 847–855.
[60] D. Sinton, Microscale flow visualization, Microfluid Nanofluid 1 (2004) 2–21.
[61] D. Ross, L.E. Locascio, Effect of caged fluorescent dye on the electroosmotic mobility in microchannels, Anal. Chem. 75 (2003) 1218–1220.
[62] H. Park, J.J. Pak, S.Y. Son, G. Lim, I. Son, Fabrication of a microchannel integrated with inner sensors and the analysis of its laminar flow characteristics, Sensors and Actuators A 103 (2003) 317–329.
[63] Y. Hu, C. Werner, D. Li, Electrokinetic transport through rough microchannels, Anal. Chem. 75 (2003) 5747–5758.